FB100 Plasma Chemical Processes

Mgr. Ondřej Jašek, Ph.D.
jasek@physics.muni.cz

PECVD at atmospheric pressure

- Plasma enhanced chemical vapor deposition with various sources
- Operation at 100 kPa without a vacuum system
- Plasma arcs, jets and torches – mostly operated in floating catalyst regime, most often used with microwave sources
- Atmospheric pressure glow discharge (APGD) diffusion form of dielectric barrier discharge (DBD) – deposition on substrates with heated electrode

Atmospheric pressure glow discharge

- Discharge configuration when one or both electrodes are covered with dielectric barrier (used for ozone production since 19th century)
- Filamentary DBD can be made diffusive with addition of He or Ne,which are both expensive gases, in can be also made homogeneous in Ar with certain hydrocarbons, N_2 or ammonia addition or special electrode structure.
- It was shown that during the current increase the discharge transits from a non-self-sustained discharge to a Townsend discharge and then to a subnormal glow discharge in He and Ar/NH3 and, therefore, can be called atmospheric pressure glow discharge (APGD).
- APGD has only 1 broad current pulse in each half period while DBD has many nanosecond current pulses, non-thermal plasma at atmospheric pressure

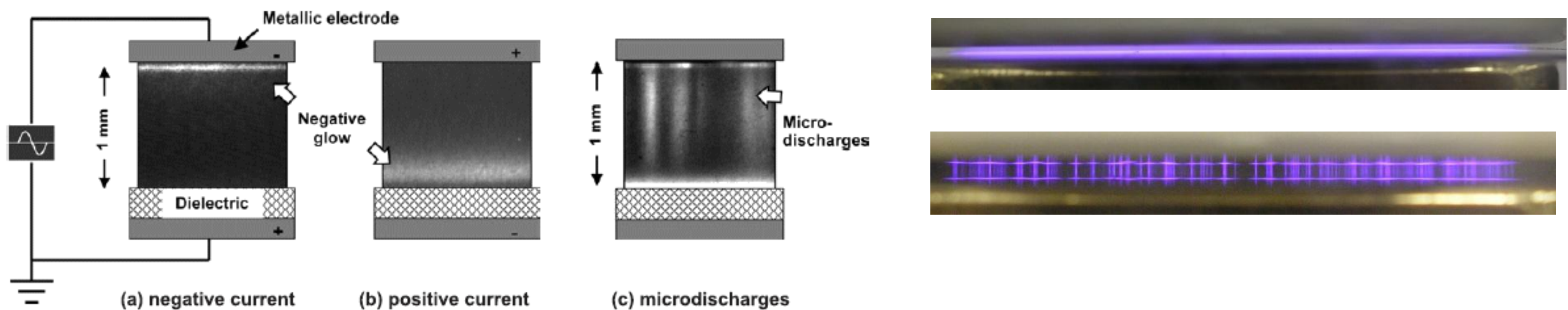

T. Nozaki, Y. Kimura and K. Okazaki, J. Phys. D: Appl. Phys. 35 (2002) 2779–2784

CNTs growth in APGD

First CNTs growth published by T. Nozaki, Y. Kimura and K. Okazaki,
J. Phys. D: Appl. Phys. 35 (2002) 2779–2784
Quartz substrate with 20 nm metal plated Ni, pretreatment in H_2 for 30 min at 600 °C
Operation in kHz mode resulted in deposition of many defective structures

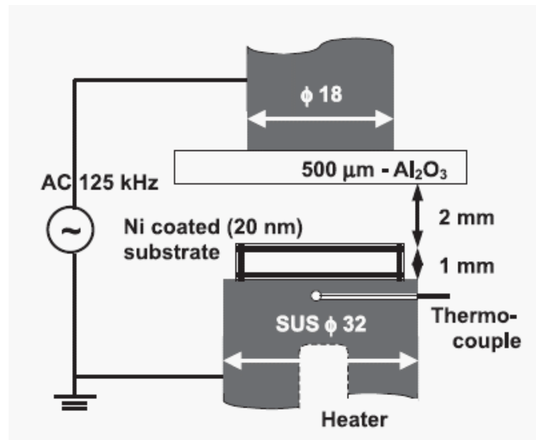

Figure 3. Electrode configuration.

Table 1. Growth parameters.

Growth temperature (°C)	400, 500, 600
Growth time (min)	5–30
H_2/CH_4 ration (-)	0, 5, 10
Flow rate of gas mixture (scc min^{-1})	APG: He : H_2 : CH_4 = 900 : 100 : 0–20 DBD: He : H_2 : CH_4 = 150 : 150 : 15
Pressure (Torr)	760
Power (current peak)	~4 W cm^{-2} (~15 mA cm^{-2})

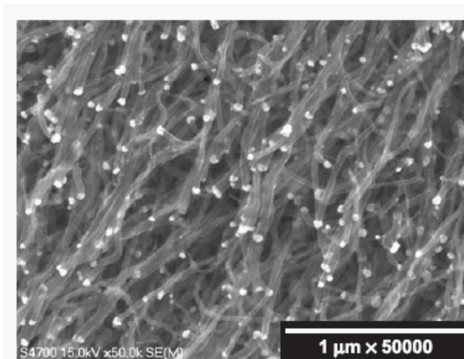

Figure 6. CNTs with uniform diameter of 40–50 nm and number density of 10^9–10^{10} cm^{-2} obtained after 30 min deposition.

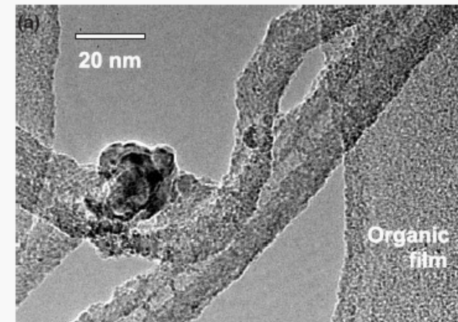

CNTs growth in APGD

- APG was also successfully used with modified electrode (pin to plate) by Y.-H. Lee, S.-H. Kyung, C.-W. Kim, G.-Y. Yeom. Carbon 44, 799 (2006) and capillary type by S.-J. Kyung, Y.-H. Lee, C.-W. Kim, J.-H. Lee, G.-Y. Yeom. Thin Solid Films 506–507, 268 (2006).

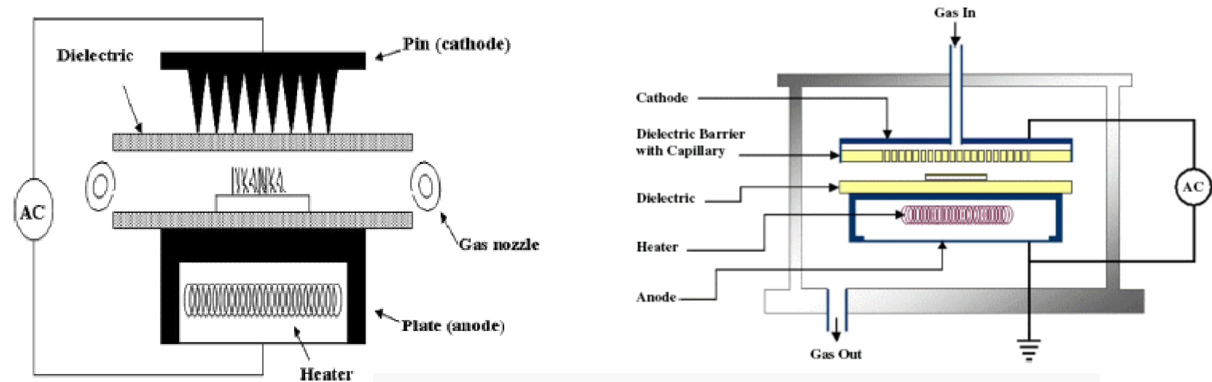

Ni (5 nm)/Cr (100 nm)/Si substrates
He(6 slm)/NH_3(90 sccm) plasma
with pretreatment at 400 °C for 5 min
He/C_2H_2(60 sccm) plasma
He/N_2(60 sccm)/C_2H_2 plasma
He/NH_3/C_2H_2 plasma
He/NH_3/C_2H_2 with dc bias 1.2 kV

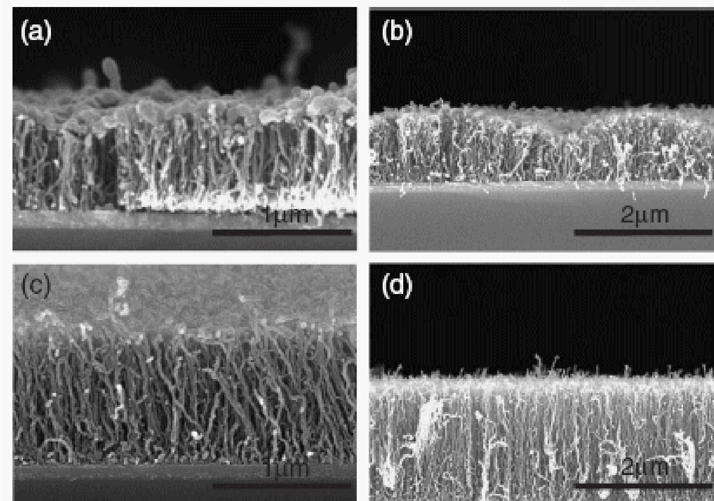

CNTs growth in APGD

- In 2006 T. Nozaki et al. J. Appl.Phys. 99, 024310 used radio-frequency power source for CNTs growth
- APRFD creates stable continuous regime for CNTs growth, much lower operating voltage due to ion “trapping” between the electrodes, no dielectric barrier needed

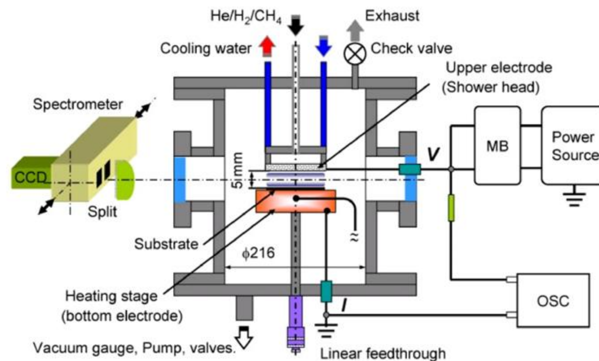

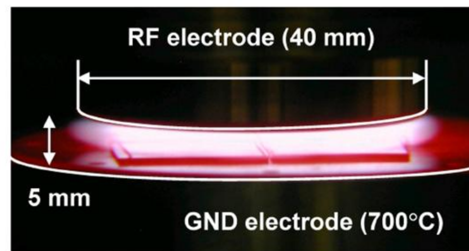

Figure 1. APRFD reactor and image of APRFD during CNT growth.

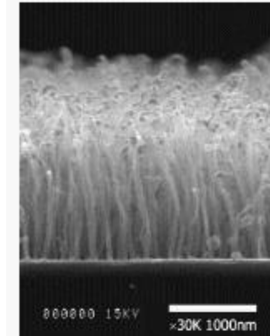

(a)

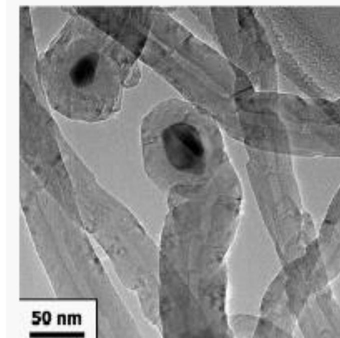

(b)

Parameters: 2 inch Si wafer <100> coated with Cr/Ni (20 nm/20 nm(sputtered)), Discharge area: 12.6 cm^2 Deposition time: 5, 10 , 20 min, $He/H_2/C_2H_2$ (1000/4-10/2 sccm)

CNTs growth in APGD

- Even with use of APRFD the growth of SWCNTs remained a challenge, key issue was the form of the catalyst
- In 2007 T. Nozaki, K. Ohnishi, K. Okazaki, U. Kortshagen. Carbon 45, 364 used densely mono-dispersed Fe–Co catalysts of a few nanometers size (first used by Maruyama) for aligned layers of SWCNTs
- Prepared nanoparticles were reduced in He/H_2 1500/10 sccm at APRFD at 400 °C for 5 min, then 15 min at 700°C, deposition $He/H_2/CH_4$ 1000/30/16 sccm for 5 min at 700 °C

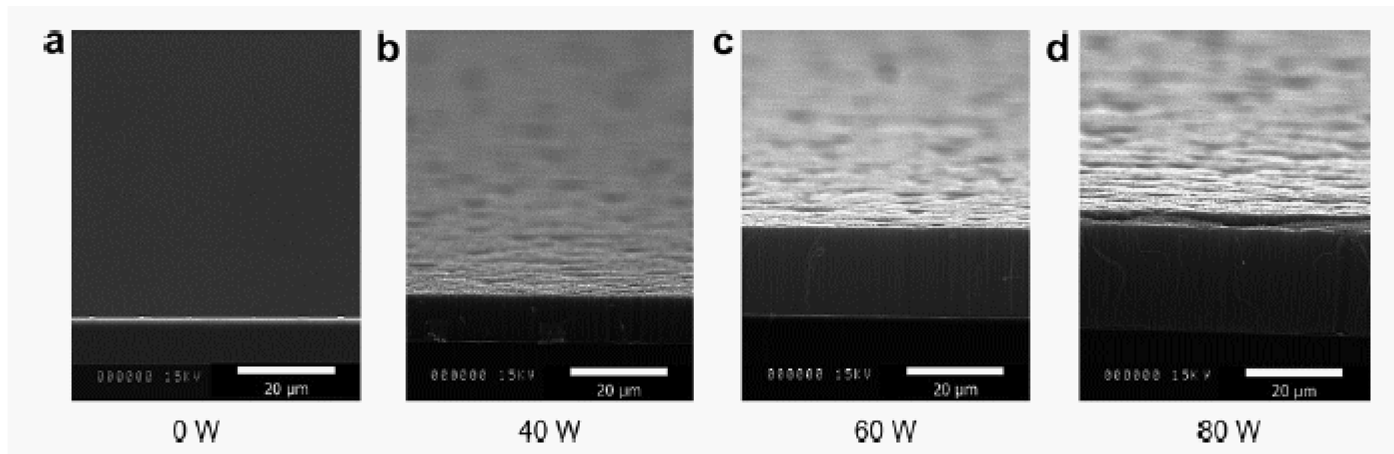

CNTs growth in APGD

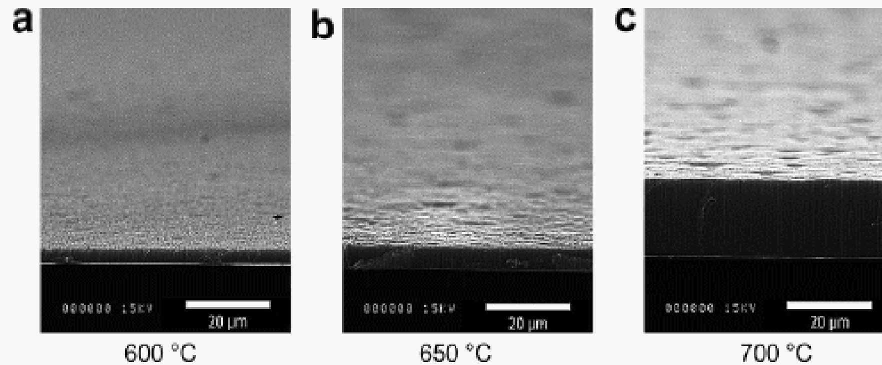

Fig. 8. SEM micrographs of SWCNTs at different substrate temperatures.

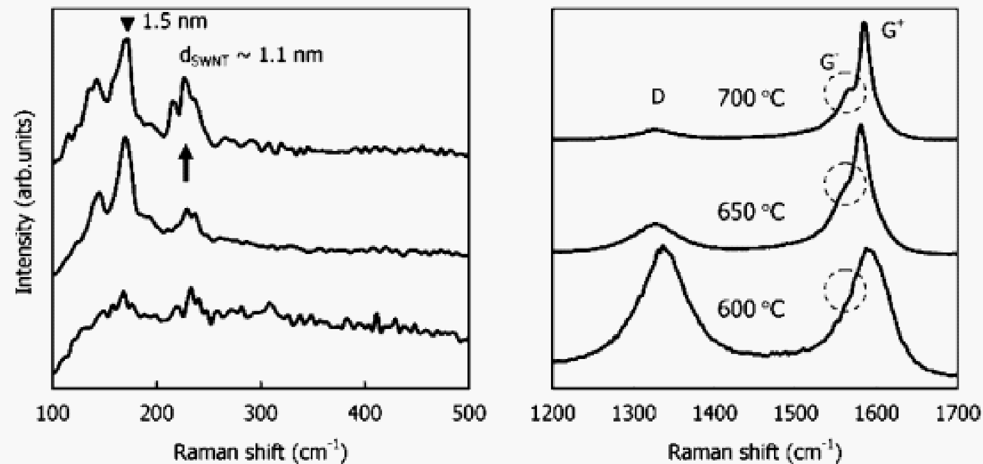

Fig. 9. Raman scattering spectra of samples shown in Fig. 8.

T. Nozaki, K. Okazaki, Carbon Nanotube Synthesis in Atmospheric Pressure Glow Discharge: A Review, Plasma Process. Polym. 2008, 5, 300–321

CNTs growth in APGD

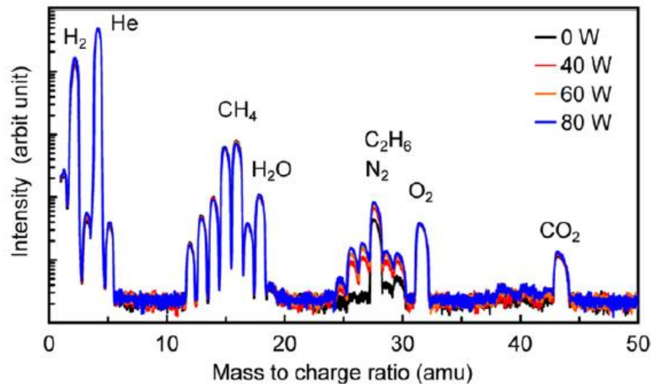

Figure 4. Mass spectrum of the reacting gas obtained directly from the sheath; conditions: $He/CH_4/H_2 = 1000/16/30\,cm^3\,min^{-1}$ and 700 °C.

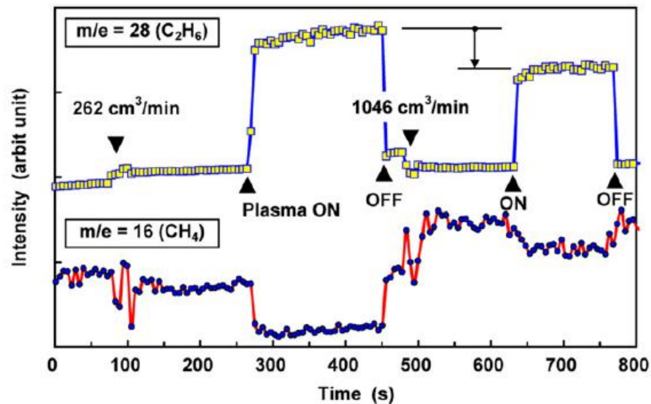

Figure 5. Time-dependent change-of-mass spectrum for $m/e = 16$ and 28. See figure 4 caption for the conditions.

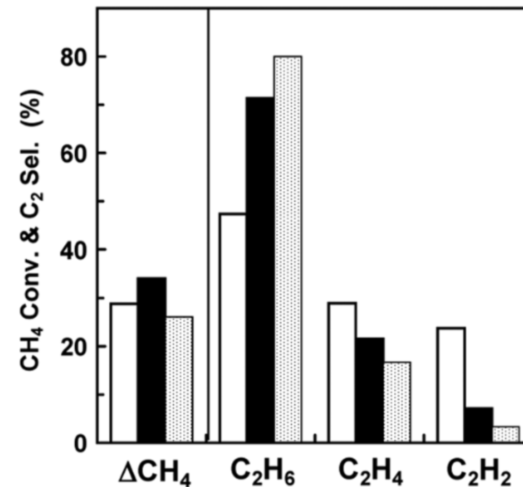

Figure 6. CH_4 conversion and selectivity for the C_2 hydrocarbon: □ 20 kPa, $H_2 = 0$; ■ 100 kPa, $H_2 = 0$; ░ 100 kPa, $H_2 = 90\,cm^3\,min^{-1}$; conditions: $He/CH_4 = 3000/48\,cm^3\,min^{-1}$ and 60 W.

T. Nozaki, S. Yoshida, T. Karatsu and K. Okazaki, Atmospheric-pressure plasma synthesis of carbon nanotubes, J. Phys. D: Appl. Phys. 44 (2011) 174007 (9pp).

CNTs growth in APG in $Ar/H_2/C_2H_2$

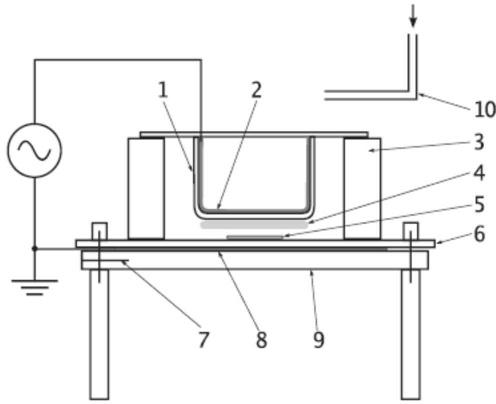

FIG. 1. Electrode configuration. 1—Simax glass dielectric, 2—upper electrode, 3—distance pillar, 4—discharge, 5—substrate, 6—AlN dielectric, 7—thermocouple, 8—bottom electrode, 9—heater, 10—gas inlet.

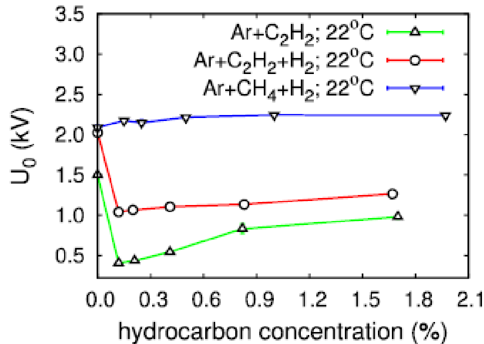

FIG. 2. The dependence of ignition voltage U_0 on the concentration or acetylene or methane added to Ar or Ar/H_2. The discharge was operated at room temperature 22 °C. Argon and hydrogen flow rates were 7 slm and 100 sccm, respectively.

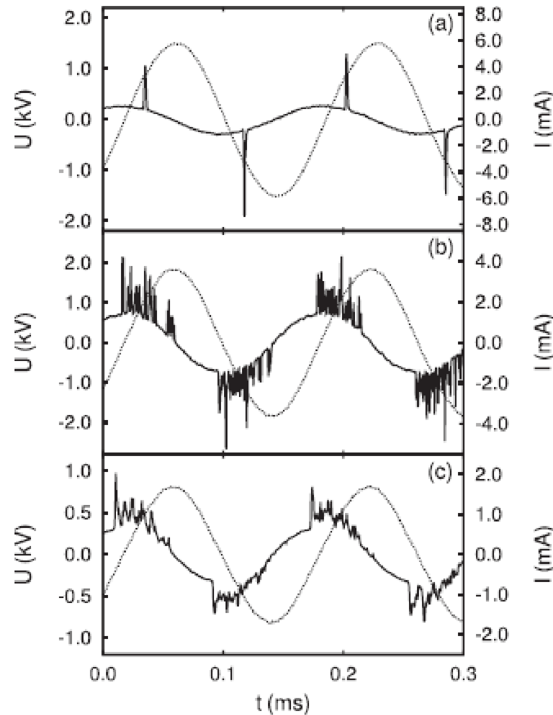

FIG. 3. The time dependence of applied voltage (dotted line) and discharge current (full line) at room temperature for (a) DBD in pure Ar, (b) DBD in Ar/CH_4, and (c) APGD in Ar/C_2H_2. The concentration of CH_4 or C_2H_2 in Ar was 0.41 vol. %. Discharges were operated slightly above the ignition voltage in particular gas mixture.

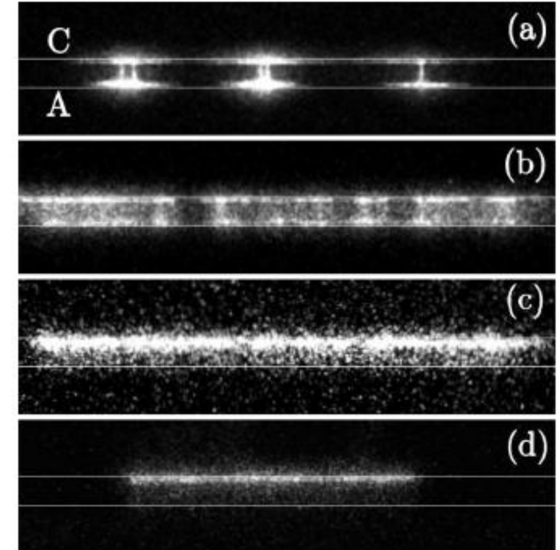

FIG. 5. ICCD images of discharges at room temperature with 80 μs (one half-period) exposure time: (a) filamentary DBD in Ar, (b) filamentary DBD in Ar/CH_4, (c) APGD in Ar/C_2H_2, and (d) APGD in Ar/C_2H_2/H_2. The concentration of CH_4 or C_2H_2 was 0.41 vol. %. Horizontal lines indicate the dielectric surfaces and the upper electrode is the instantaneous cathode in all images.

6,8 kHz power supply with 0.8–4.0 kV (peak-to-peak) voltage , electrode distance of 1,75 mm, 10x15 mm Si/SiO2 (300 nm)/5 nm Fe catalytic layer. Ar/H2/CH_4 or C_2H_2 mixture.

Eliáš M., Kloc P., Jašek O., Mazánková V., Trunec D., Hrdý R., Zajíčková L., Atmospheric pressure barrier discharge at high temperature: Diagnostics and carbon nanotubes deposition, Journal of Applied Physics 117(10) (2015) 103301.

CNTs growth in APG in $Ar/H_2/C_2H_2$ – diagnostics at high temperature

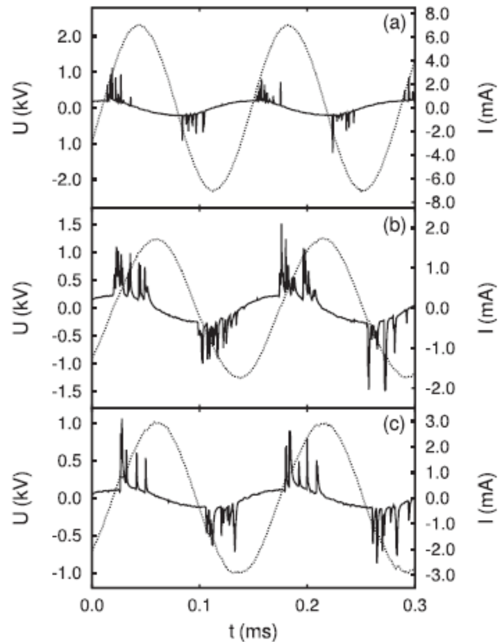

FIG. 4. The time dependence of applied voltage (dotted line) and discharge current (full line) for (a) DBD in $Ar/CH_4/H_2$ at 22 °C, (b) APGD $Ar/C_2H_2/H_2$ at 22 °C, and (c) APGD $Ar/C_2H_2/H_2$ at 680 °C. The concentration of CH_4 or C_2H_2 in Ar/H_2 was 0.41 vol. %. Discharges were operated slightly above the ignition voltage in particular gas mixture.

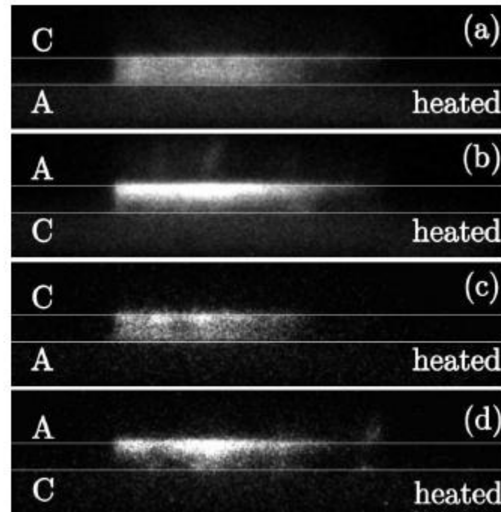

FIG. 8. ICCD images of APGD in $Ar/C_2H_2/H_2$ with 0.41 vol. % admixture of C_2H_2 and bottom electrode heated to 680 °C: (a) 80 μs (one half-period), instantaneous cathode at upper electrode, (b) 80 μs (one half-period), cathode at bottom electrode, (c) 5 μs, cathode at upper electrode, and (d) 5 μs, cathode at bottom electrode. Horizontal lines indicate the dielectric surfaces.

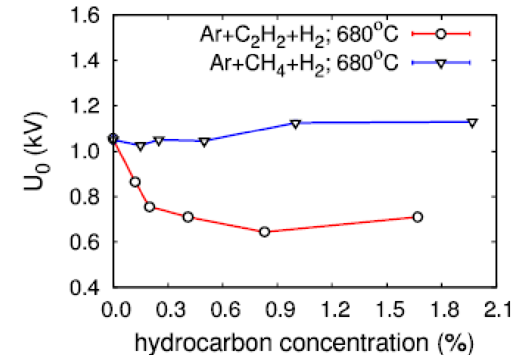

FIG. 7. The ignition voltage U_0 in dependence on the concentration of acetylene or methane added to Ar/H_2 for the temperature of bottom electrode 680 °C. Argon and hydrogen flow rates were 7 slm and 100 sccm, respectively.

If the bottom electrode was heated up to 680 °C the ignition voltage decreases due to the decrease of neutral gas concentration. Substrate temperature is 40 °C lower then heated electrode and upper electrode temperature is 250 °C lower. Due to the temperature profile the behaviour in instantaneous cathode or anode is different in each half period.

CNTs growth in APG in $Ar/H_2/C_2H_2$

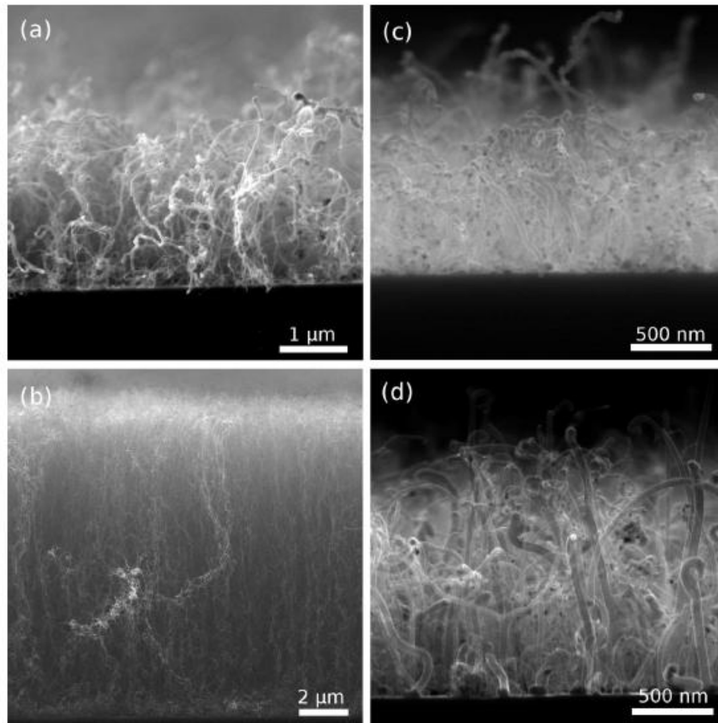

FIG. 13. Cross sectional SEM micrographs of deposited carbon nanostructures for (a) 0.1%, (b) 0.2% of C_2H_2 in $Ar/C_2H_2/H_2$ APG discharges, and (c) 0.2%, (d) 0.4% of CH_4 in $Ar/CH_4/H_2$ DBD discharges. The substrate temperature was 710 °C. The micrographs were made using TESCAN LYRA microscope.

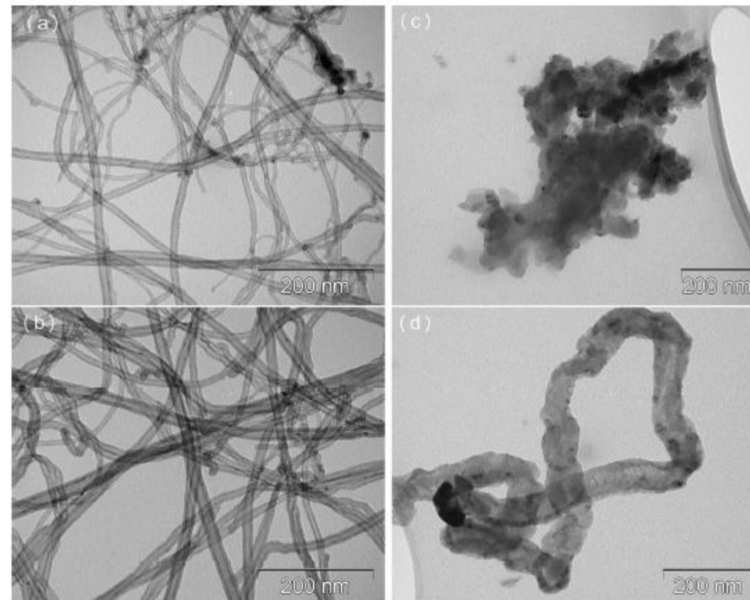

FIG. 12. TEM micrograph of the carbon nanostructures deposited from (a), (b) 0.2% of C_2H_2 in $Ar/C_2H_2/H_2$ mixture and (c), (d) 0.2% of CH_4 in $Ar/CH_4/H_2$ mixture. The substrate temperature was 610 °C for (a) and (c) and 710 °C for (b) and (d) images. The micrographs were made using Philips CM12 microscope.

CNTs deposition by plasma arcs/jets/torches at atmospheric pressure

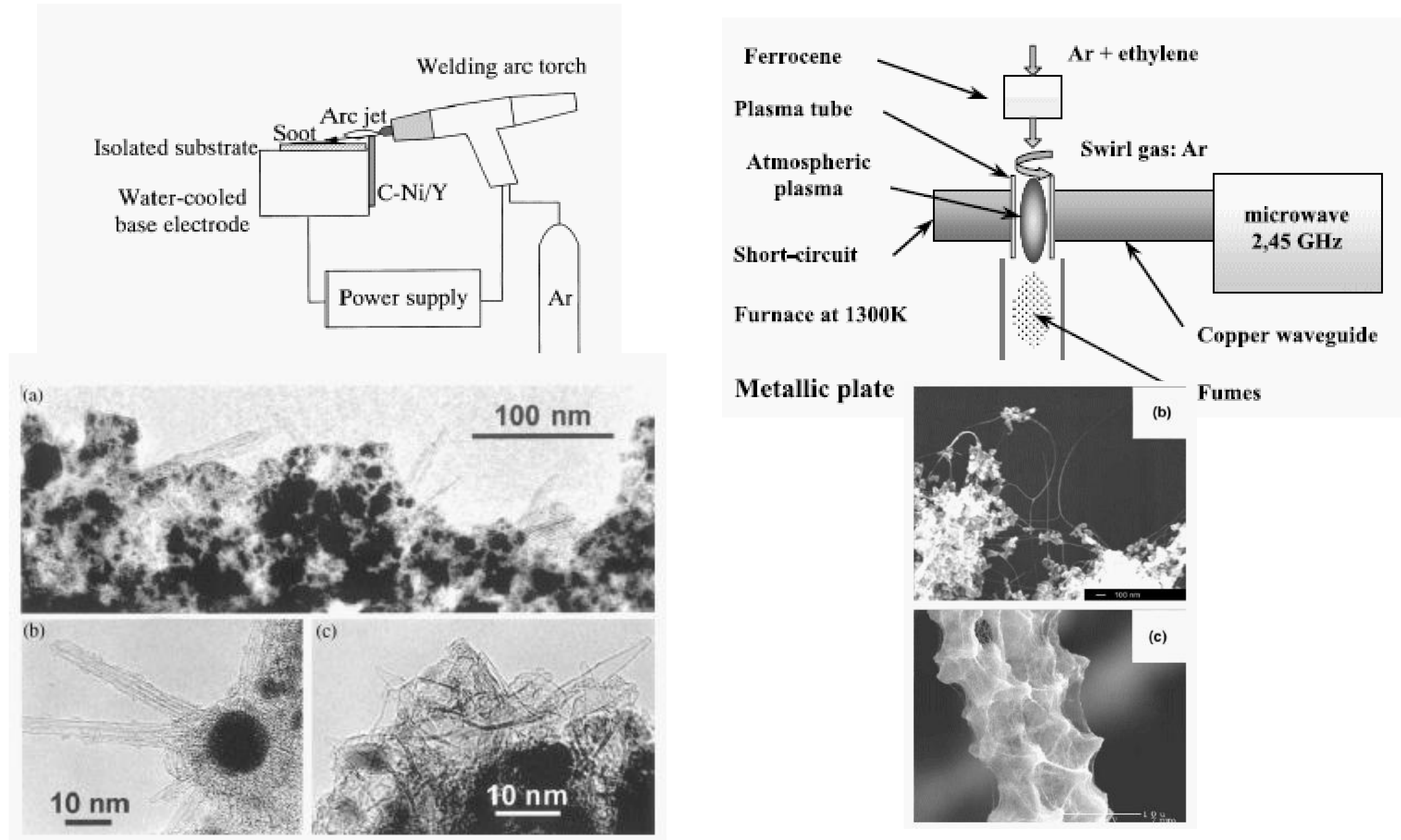

H. Takikawa et al. *Physica B* 323, 277 (2002)., O. Smiljanic et al., Chem. Phys. Lett. 356, 189 (2002).

CNTs deposition by plasma arcs/jets/torches at atmospheric pressure

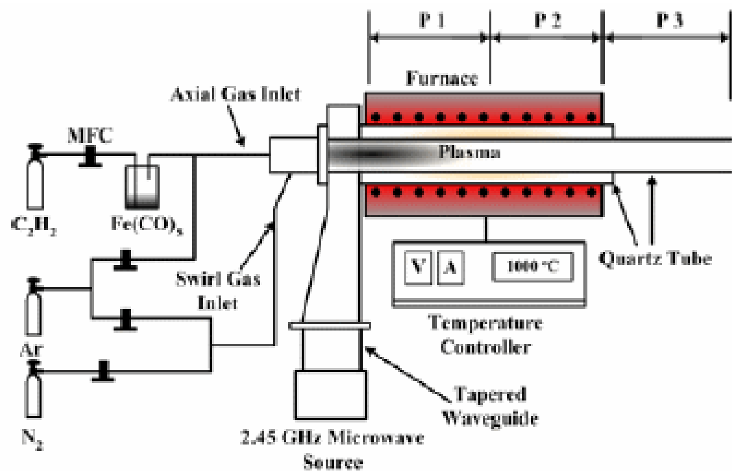

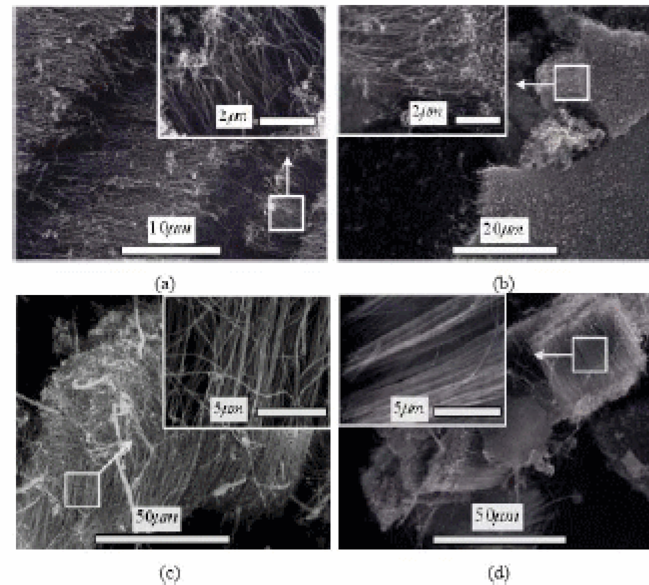

Fig. 9. SEM images of CNTs obtained from the atmospheric microwave plasma-torch. (a) at a furnace temperature of 700, (b) 800, (c) 900, and (d) 1000 °C.

Y. Ch. Hong, H. S. Uhm, Physics of plasmas 12, 053504 (2005)

CNTs synthesis by microwave plasma torch at atmospheric pressure

Microwave plasma torch operating at 2,45 GHz, max. 2 kW power, dual gas flow
Center - Ar(500-1500 sccm)/
Outer - H_2(250-500 sccm)/CH_4(10-50 sccm)
Si/Fe, Si/SiO_x/Fe, Si/Al_xO_y/Fe substrates
Fe(1-10 nm) vacuum evaporated, SiO_x PECVD
O. Jašek, M. Eliáš, L. Zajíčková et al., Materials Science and Eng. C, 26, 2006, 1189

CNTs synthesis by microwave plasma torch at atmospheric pressure

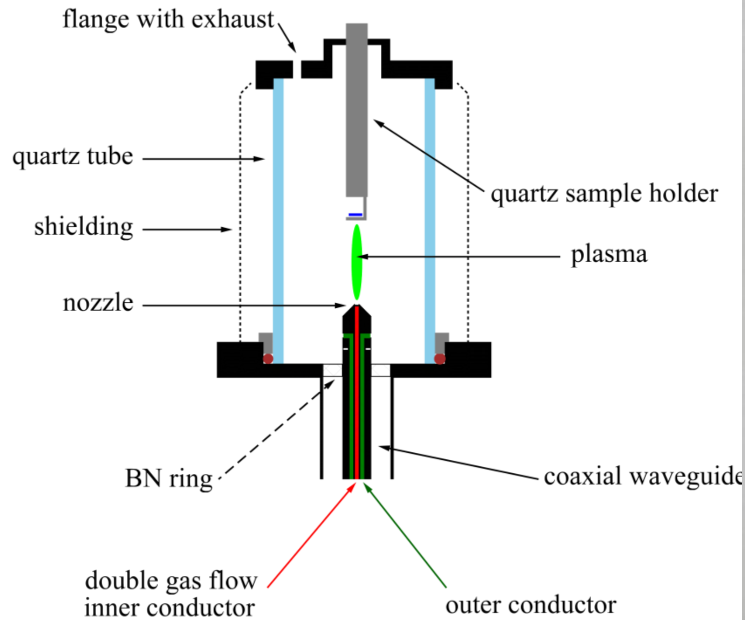

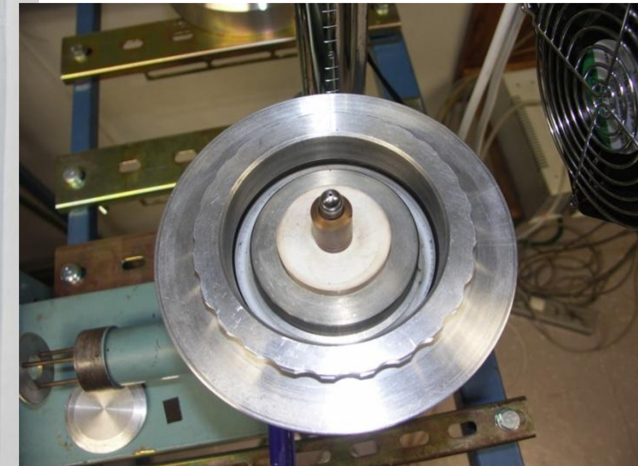

CNTs synthesis by microwave plasma torch at atmospheric pressure

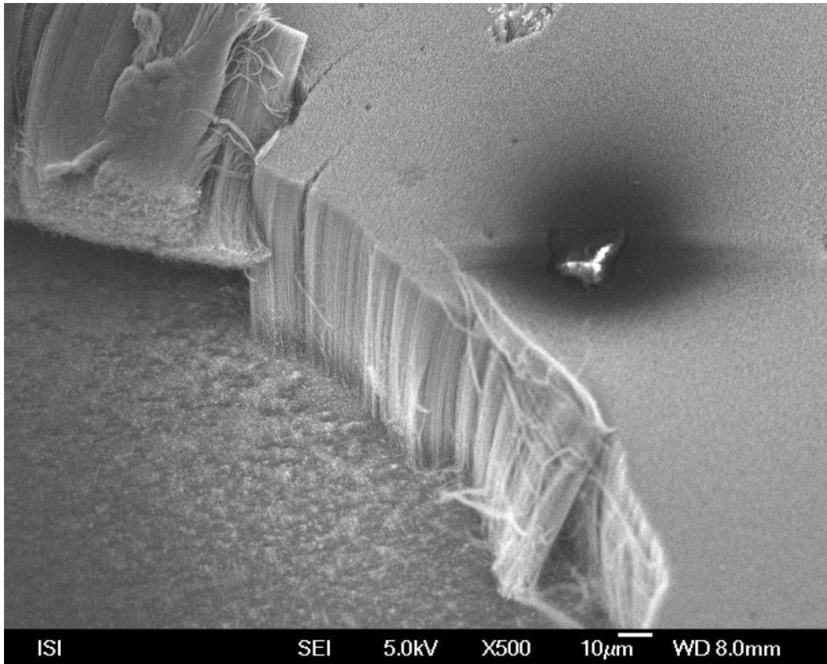

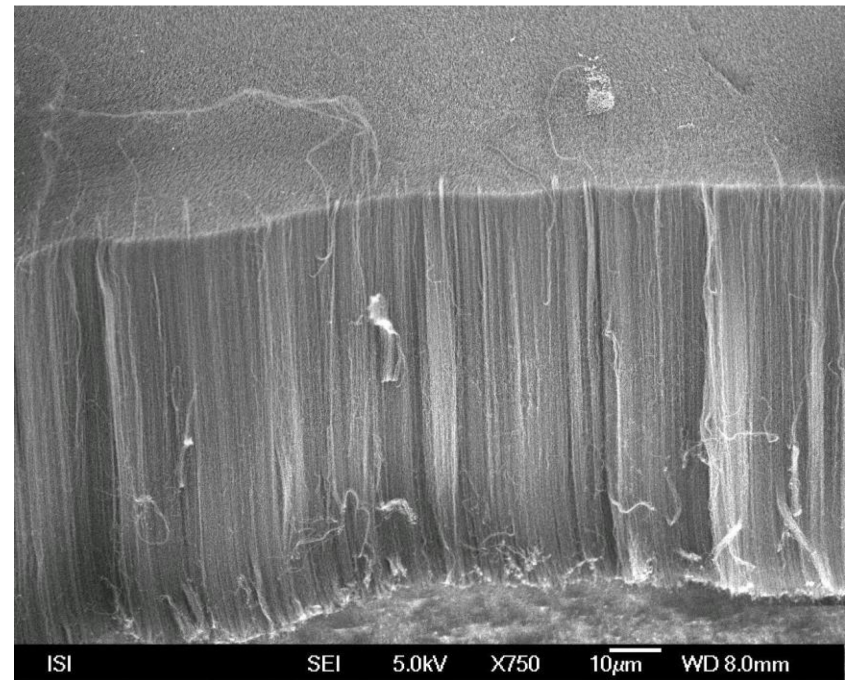

Substrate type Si/SiO$_2$/Fe 10 nm (Q_{CH4}=40 sccm, Q_{H2}=400 sccm, Ar=1500 sccm, T_S=700^{0}C, t_d=15 min.).

CNTs synthesis by microwave plasma torch at atmospheric pressure

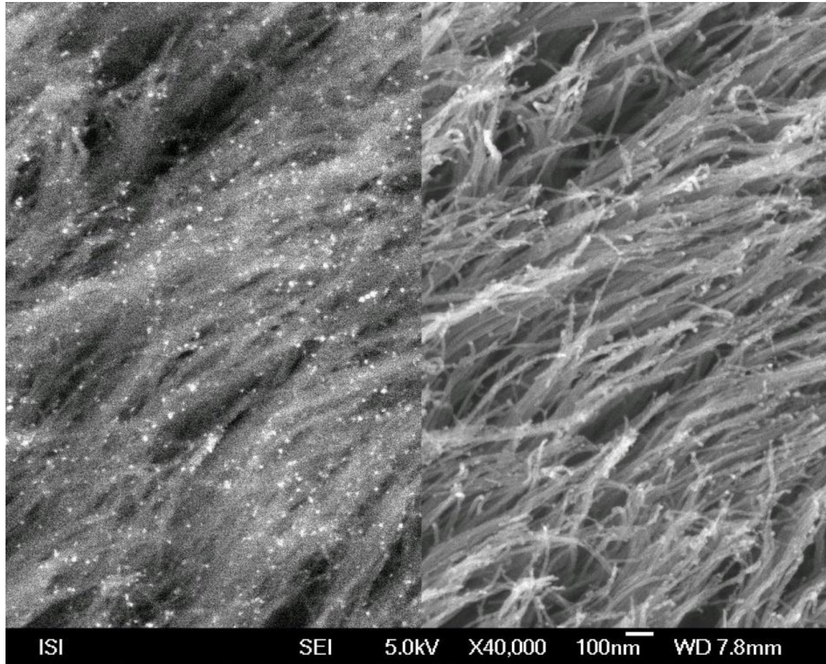

Material contrast analysis – comparison of micrographs in secondary and backscattered electrons. White points correspond to catalytic particles – tip growth mode.

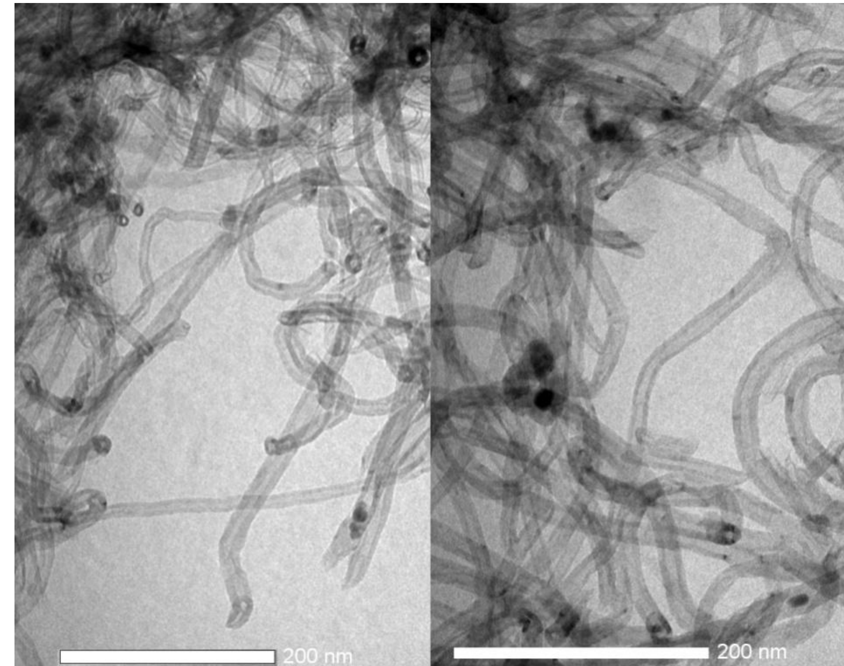

TEM micrograph

CNTs synthesis by microwave plasma torch at atmospheric pressure

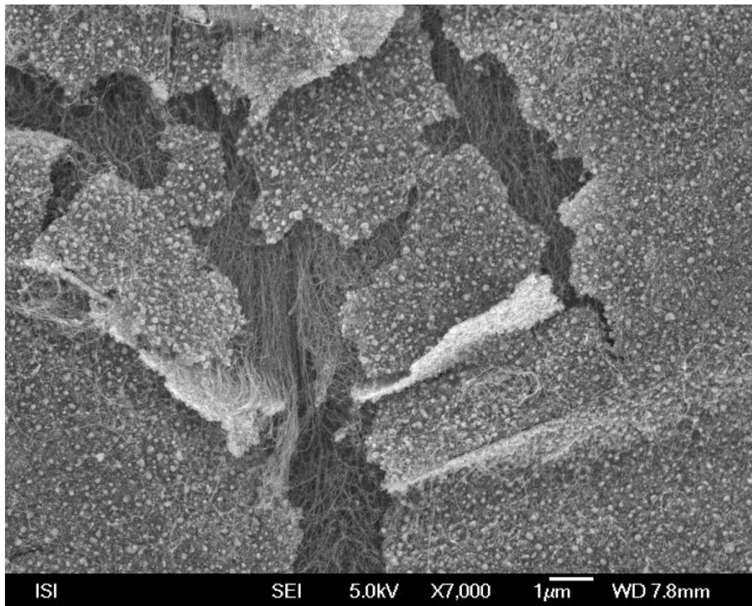

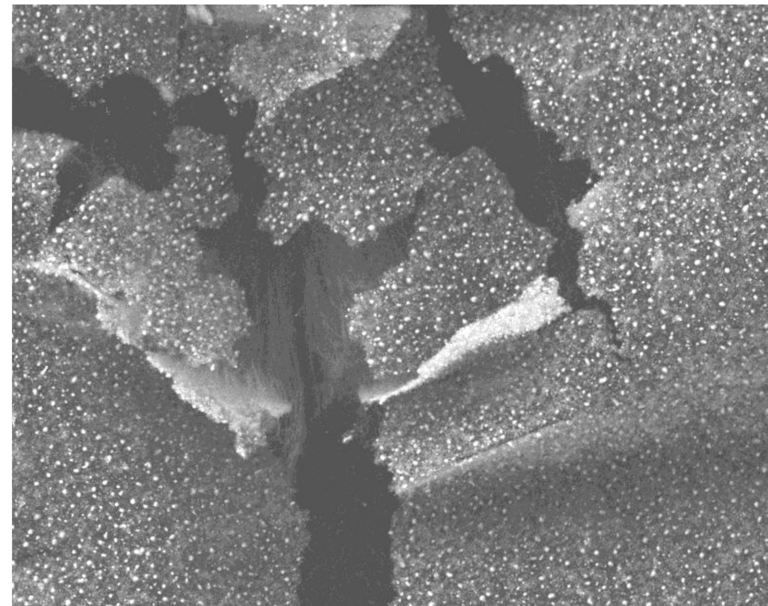

Growth termination and overlayer formation

CNTs synthesis by microwave plasma torch at atmospheric pressure

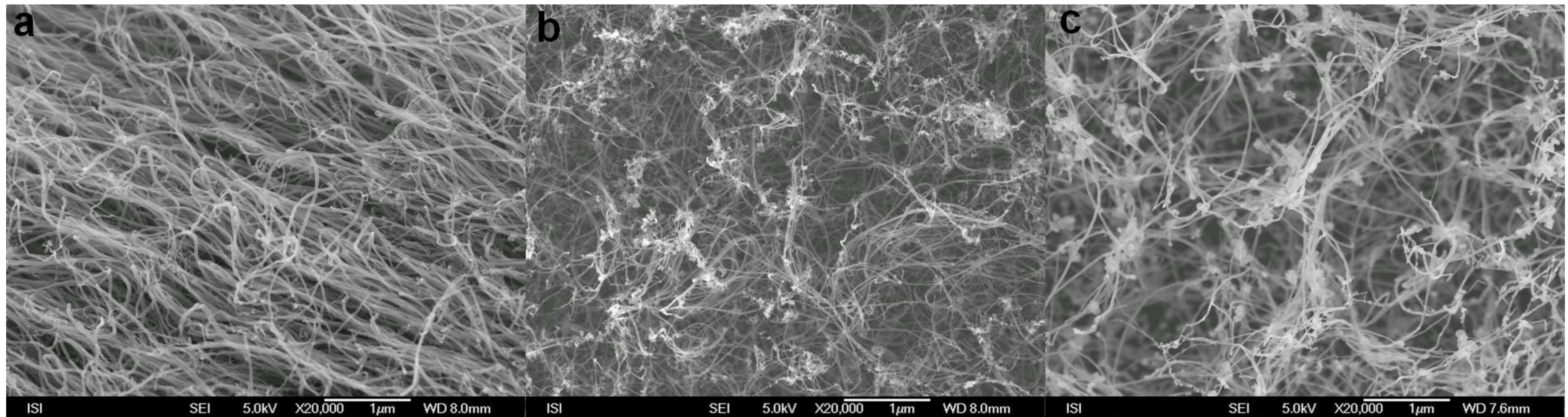

CNTs growth a) SiO_x b) Al_xO_y and c) without barrier layer.
$Ar/H_2/CH_4$ 1540/430/42 sccm, 60 s, 400W, 700-750 °C

CNTs synthesis by microwave plasma torch at atmospheric pressure

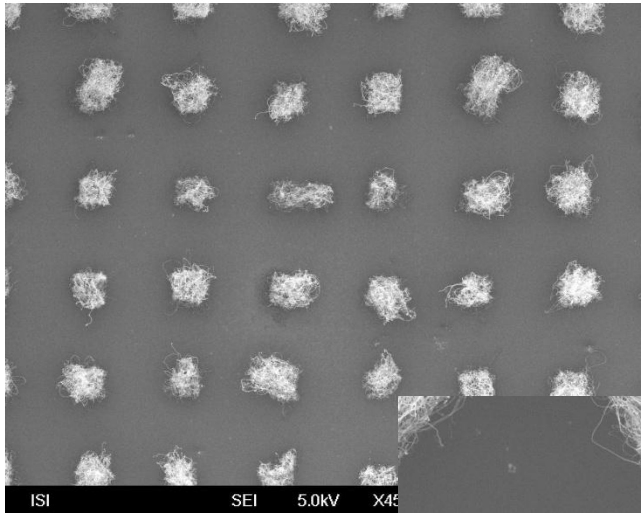

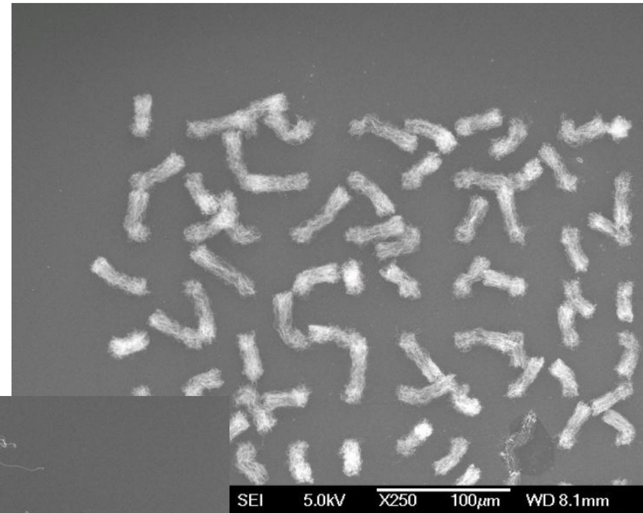

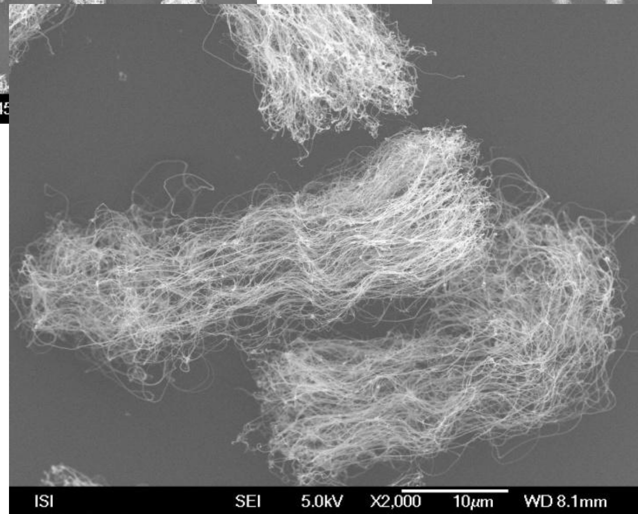

Growth pattering without barrier layer

CNTs growth in microwave plasma torch with floating catalyst

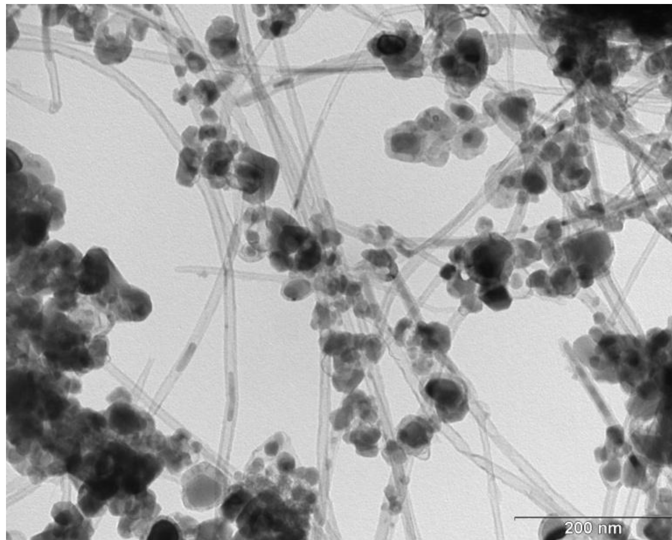

TEM micrograph of MWCNTs/SWCNTs deposited from mixture of $Ar/H_2/CH_4$ and $Fe(CO)_5$
Deposition of SWCNTs on the substrate using ethanol admixture

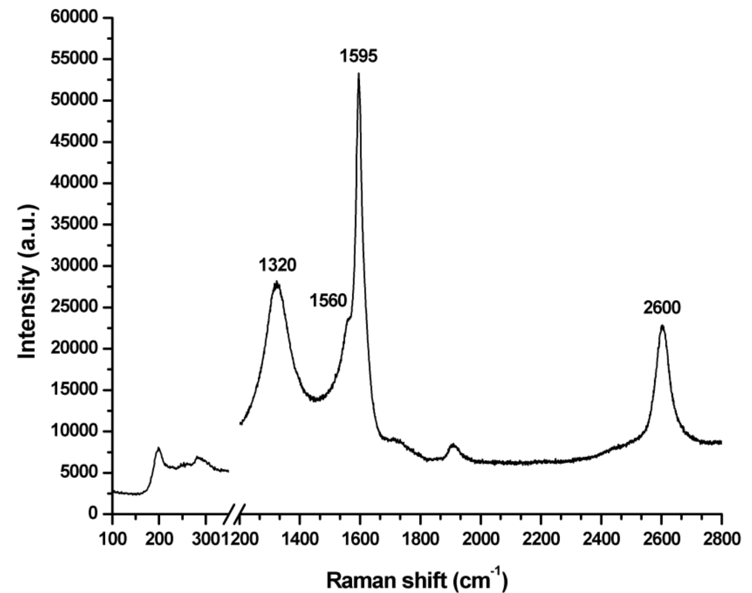

Raman spectra of deposited nanostructures

Various forms of carbon

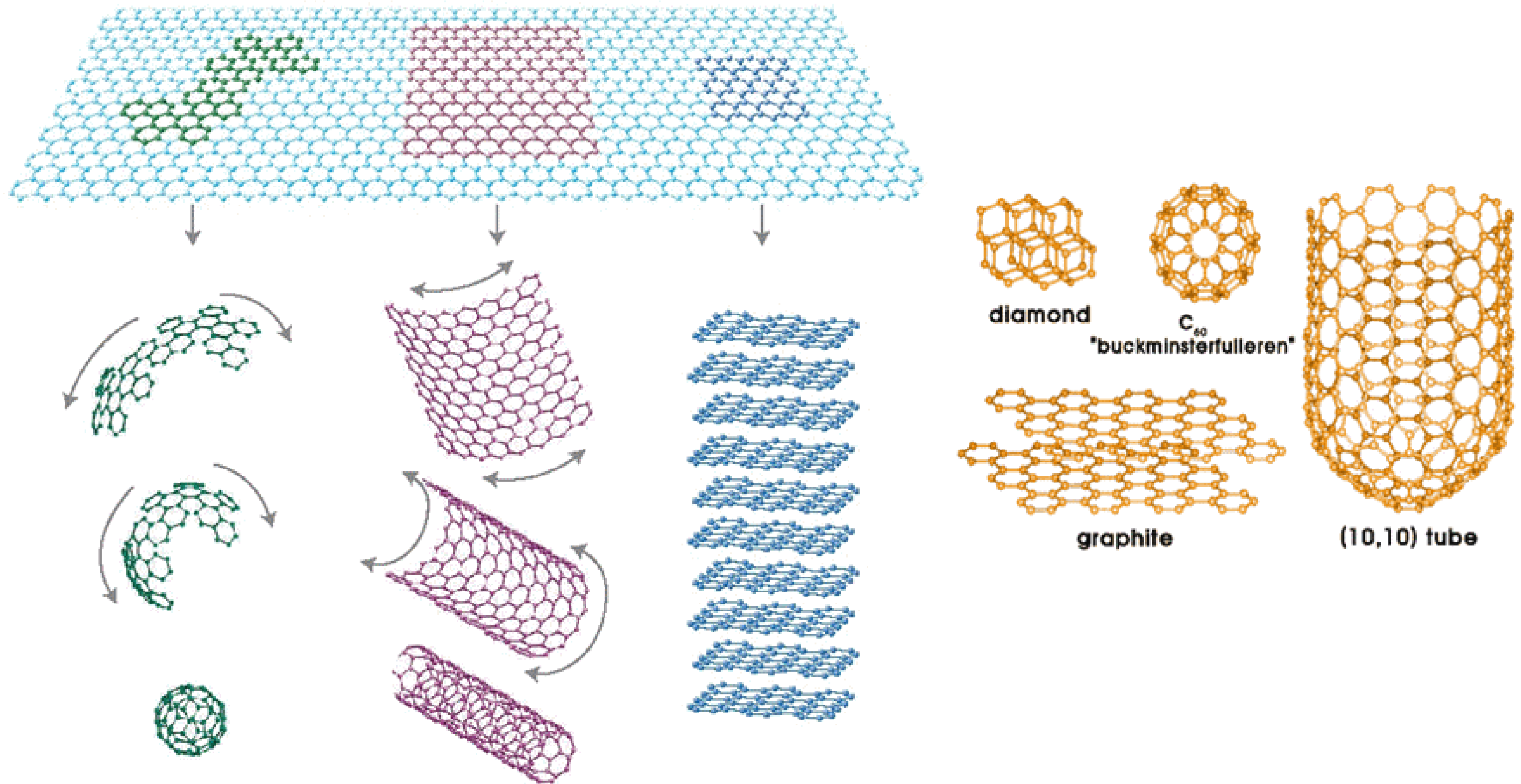

Methods of making graphene

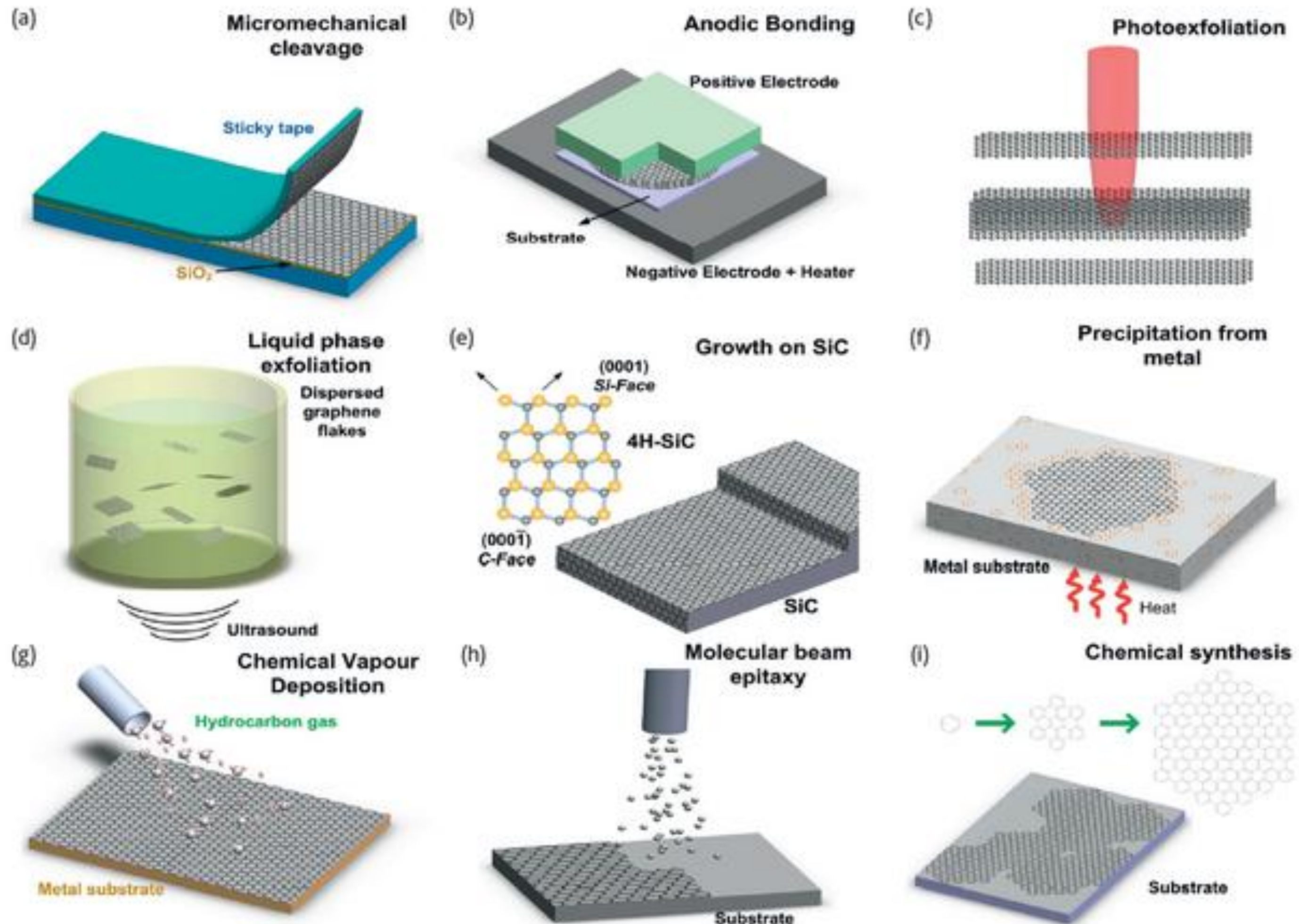

F. Bonaccorso et. al. Production and processing of graphene and 2d crystals, Materials Today 15(12), 2012, 564

Graphene identification in Raman spectra

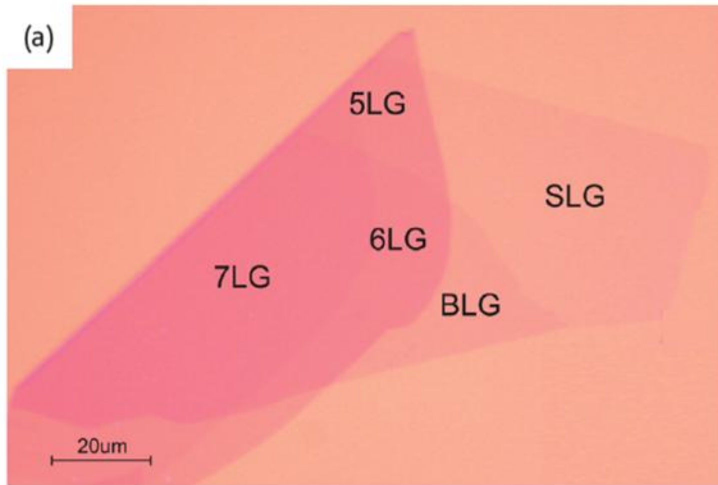

Optical contrast on SiO_2, best around 300 nm thickness.

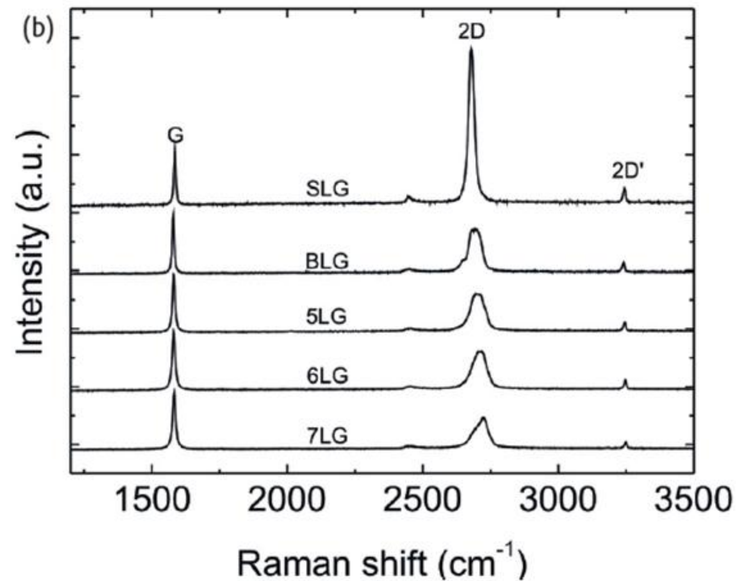

Highly sensitive Raman signal – strong enhancement of 2D mode.
No defects – no D peak around 1300 cm^{-1}.

Graphene deposition using plasma sources

- Synthesis in volume of the plasma discharge
- Synthesis of vertical aligned graphene nanosheets on substrates
- Synthesis of graphene on metalic or dielectric substrates by PECVD
- Plasma pretreatment, cleaning of the substrate, functionalization of the deposition layer – graphane (H_2), graphene transfer

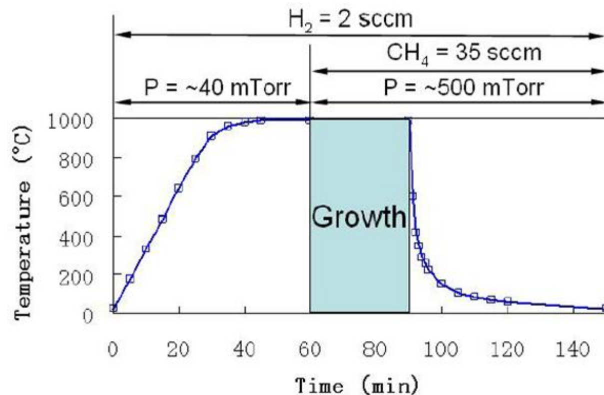

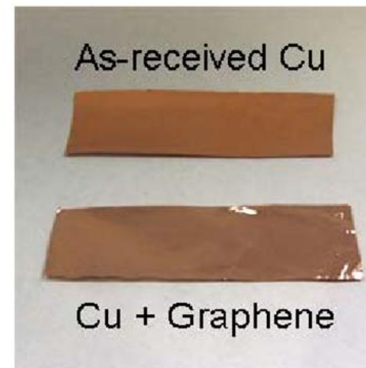

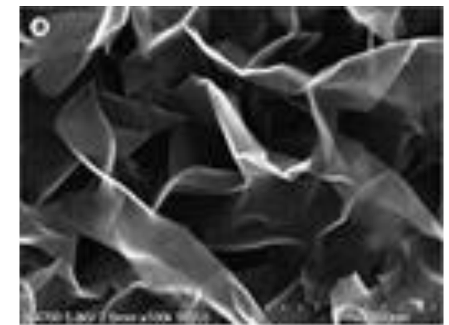

Graphene deposition using plasma sources

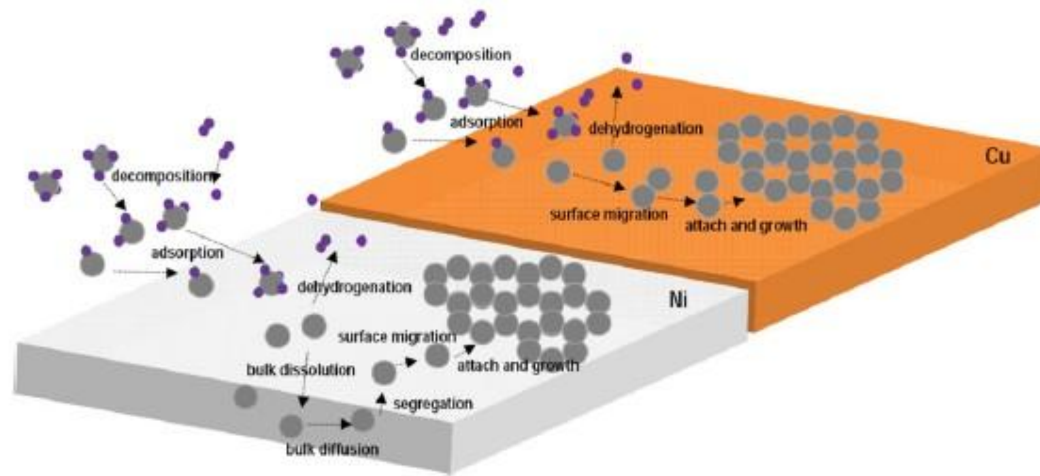

Fig. 2. Growth kinetics in CVD-produced graphene on various catalysts: Case of CH_4 on Ni and Cu.

R. Munoz and C. Gomez-Aleixandre, Review of CVD Synthesis of Graphene, Chem. Vap. Deposition 2013, 19, 297

Graphene deposition using plasma sources

Low pressure microwave plasma surface wave discharge.
Cu (30 μm),Al (12 μm), Ni foils pretreated in Ar/H_2 plasma at 5 Pa for 20 minutes. Deposition parameters: 3-4.5 kW MW power, deposition time 30-180 s in CH4/Ar/H2 30/20/10 sccm mixture.

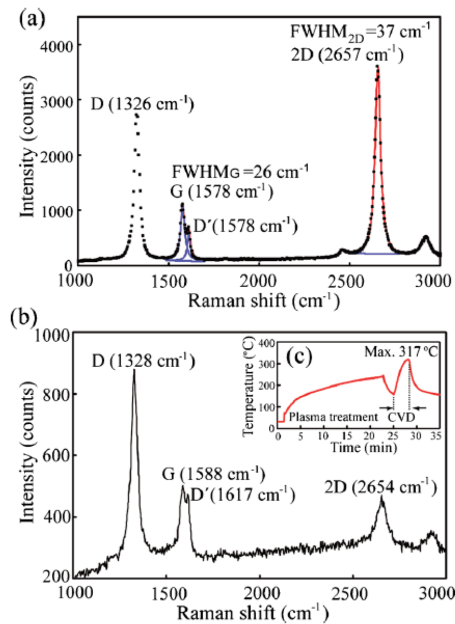

FIG. 1. (Color online) Raman spectra (638 nm laser, 1 μm spot size) o graphene-based films deposited at substrate temperatures below 400 °C b SWP-CVD. (a) Raman spectrum of a typical graphene-based film deposite on Cu foil (CVD conditions: 5 Pa, $CH_4/Ar/H_2$=30/20/10 SCCM, 3 kW per a MW generator, 30 s). (b) Raman spectrum of a graphene-base film deposited on Al foil (CVD conditions: 3 Pa, $CH_4/Ar/H$ =30/20/10 SCCM, 4 kW per a MW generator, 180 s). (c) Substrate tem perature profile during the Ar/H_2 plasma treatment and the plasma CVD fo the synthesis of the film on Al foil shown in Fig. 1(b).

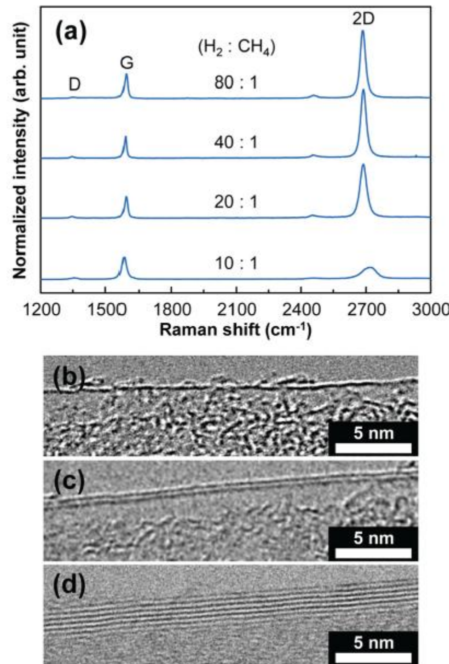

FIG. 1. (Color online) (a) Raman spectra taken at an excitation wavelength of 514 nm for the graphene films synthesized at various gas mixing ratio (synthesis time: 1 min, temperature: 750 °C). HR-TEM images of the graphene films synthesized at various gases mixing ratio: (b) 80:1 (H_2:CH_4), (c) 40:1, and (d) 10:1.

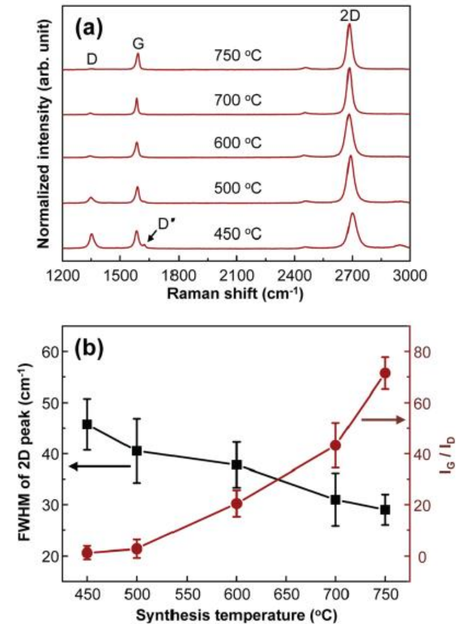

FIG. 2. (Color online) (a) Raman spectra taken at an excitation energy of 2.41 eV for the graphene synthesized at several synthesis temperatures (gas mixing ratio (H_2:CH_4): 80:1, synthesis time: 1 min). (b) FWHM of the 2D peak and the intensity ratio of the 2D peak compared to the G peak as a function of synthesis the temperature.

Y. Kim et al, Low-temperature synthesis of graphene on nickel foil by microwave plasma chemical vapor deposition, APPLIED PHYSICS LETTERS 98, 263106 (2011).
J. Kim et al., Low-temperature synthesis of large-area graphene-based transparent conductive films using surface wave plasma chemical vapor deposition, APPLIED PHYSICS LETTERS 98, 091502 2011.

Graphene deposition using plasma sources

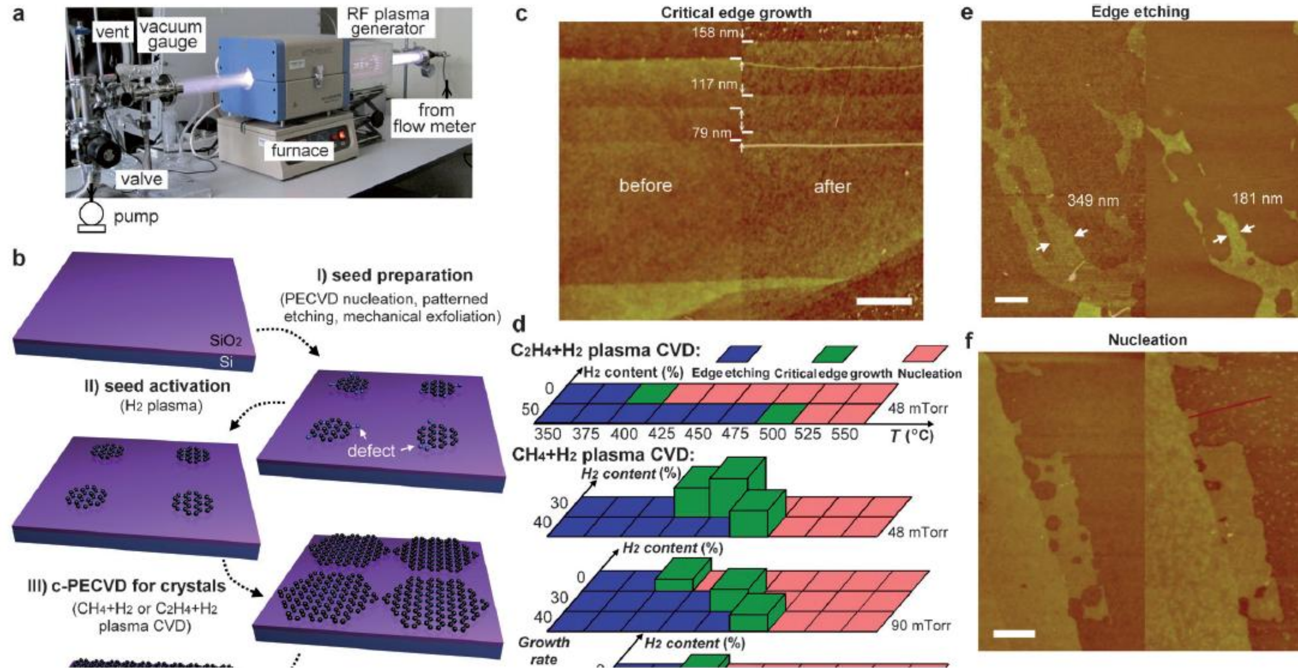

Figure 1. a) The remote radiofrequency (RF) PECVD system used. b) Schematic illustration of the c-PECVD procedure. c) AFM images of a peel-off graphene flake before (left) and after (right) c-PECVD. d) Plots of the experimental results as a function of the temperature (*T*) and H_2 content at 48, 90, and 300 mTorr. The blue, green, and red areas correspond to the parameters for edge etching, critical edge growth, and cluster nucleation, respectively. The height of the green columns indicates the growth rate. e,f) AFM images of peel-off graphene flakes after activation of the edges with a H_2 plasma (250 mTorr, 500°C) for 20 min (left columns), followed by CH_4+H_2 plasma CVD (30% H_2, 300 mTorr, 550°C) for 80 min (e, right column) or CH_4+H_2 plasma CVD (20% H_2, 300 mTorr, 600°C) for 40 min (f, right column). The height profile across the red line in the AFM image in (f) is shown below the AFM image. Scale bars (c,e,f): 500 nm.

RF PECVD remote plasma system with furnace and Si/SiO_2 substrate
D. Wei et al., Critical Crystal Growth of Graphene on Dielectric Substrates at Low Temperature for Electronic Devices, Angew. Chem. Int. Ed. 2013, 52, 14121 –14126.

Graphene deposition using plasma sources

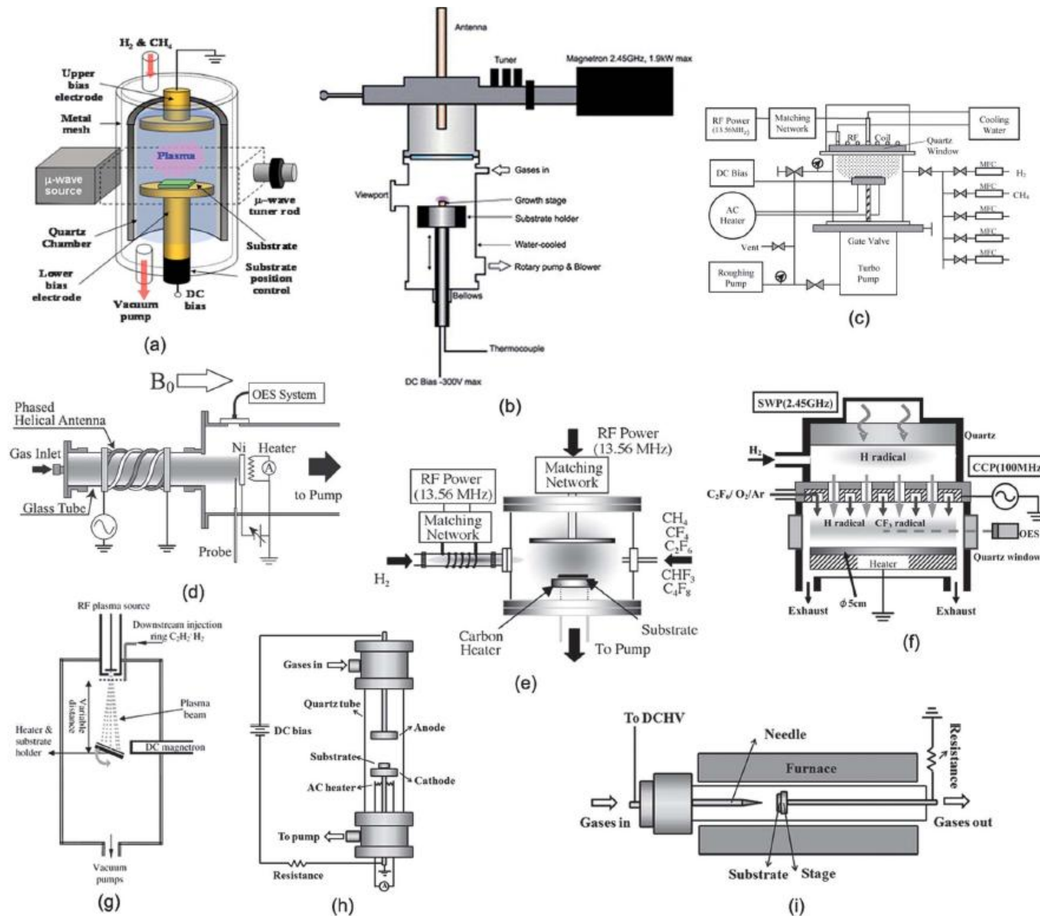

Fig. 1 Schematic diagrams of various PECVD systems for VG growth: (a) TE-MW (reprinted with permission from ref. 67; Copyright 2010 American Institute of Physics), (b) TM-MW (reprinted with permission from ref. 25; Copyright 2006 Elsevier), (c) ICP (reused with permission from ref. 68; Copyright (2004) Elsevier), (d) helicon plasma (reprinted with permission from ref. 24; Copyright 2006 Japan Society of Applied Physics), (e) CCP + ICP (reused with permission from ref. 69; Copyright 2005 Elsevier), (f) VHFCCP + MW (reprinted with permission from ref. 29; Copyright 2008 American Institute of Physics), (g) expanding CCP (reprinted with permission from ref. 70; Copyright 2010 Institute of Physics Publishing), (h) parallel-plate dc glow discharge plasma, and (i) pin-to-plate normal glow discharge plasma.

Z. Bo et al., Plasma-enhanced chemical vapor deposition synthesis of vertically oriented graphene nanosheets, Nanoscale, 2013, 5, 5180.

Graphene deposition using plasma sources

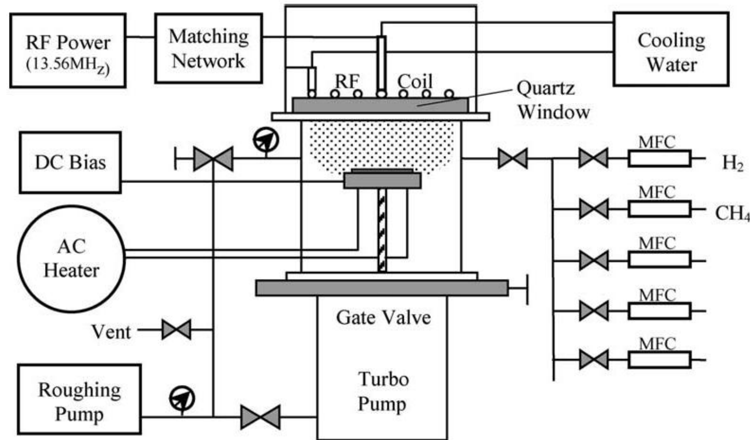

Fig. 1. Schematic of the inductively coupled RF PECVD system used for carbon nanosheet depositioı

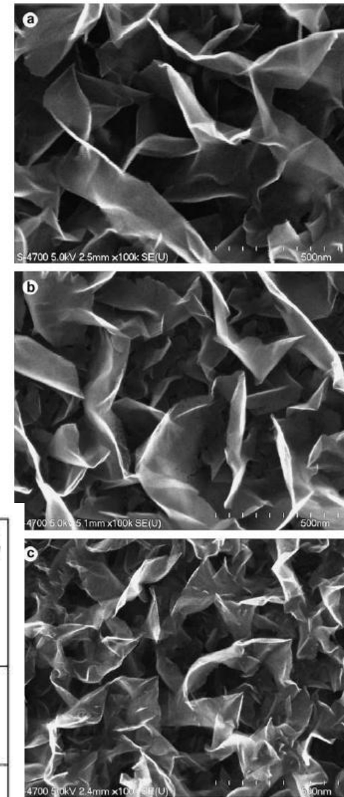

ΞM images of carbon nanosheets grown at different CH_4 tions on Si substrates: (a) 10% CH_4; (b) 40% CH_4; (c) 100% er deposition conditions are RF 900 W, 680 °C, ~12 Pa,

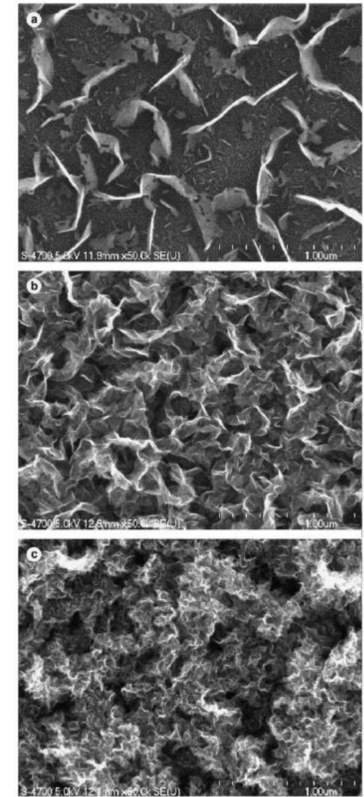

Fig. 3. SEM images of carbon nanosheets grown at different substrate temperatures on Si substrates: (a) 630 °C; (b) 730 °C; (c) 830 °C. Other deposition conditions are RF 900 W, 40% CH_4, 12 Pa, 20 min.

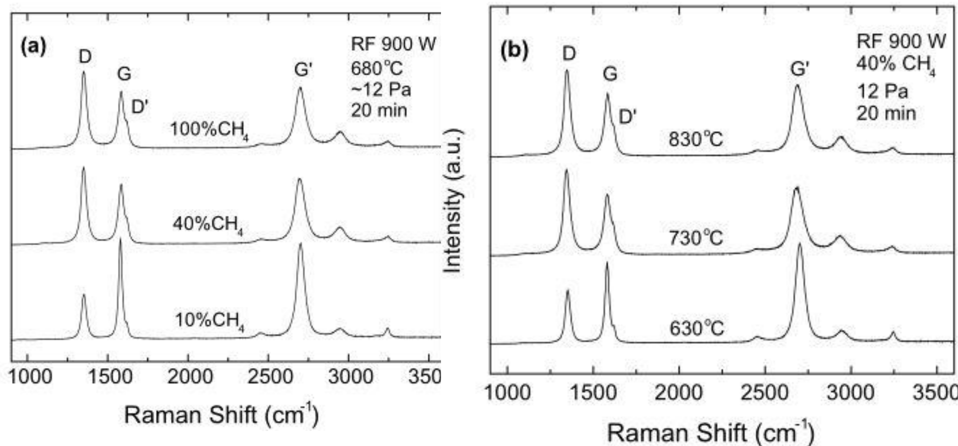

J. Wang et.al. Synthesis of carbon nanosheets by inductively coupled radio-frequency plasma enhanced chemical vapor deposition, Carbon 42 (2004) 2867–2872.

RF ICP CVD 13,56 MHz 900 W, 12 Pa, H_2/CH_4 mixture . Substrate Si, SiO_2, Al_2O_3, Mo, Cu etc.

Graphene synthesis in volume at atmospheric pressure

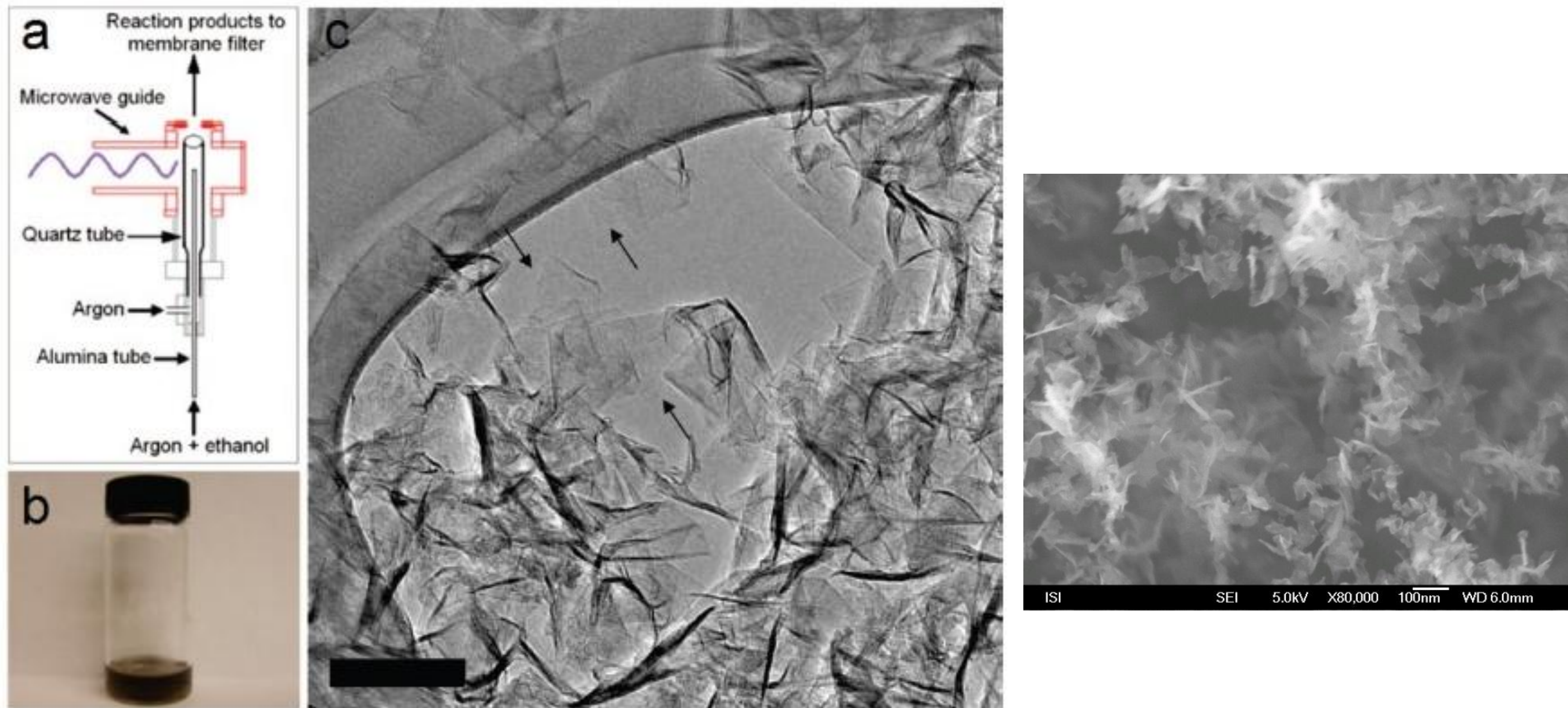

Decomposition of ethanol C_2H_5OH or dimethylether CH_3OCH_3 leads to formation of graphene sheets.

A. Dato, V. Radmilovic, Z. Lee, J. Phillips, and M. Frenklach, Substrate-Free Gas-Phase Synthesis of Graphene Sheets, Nano Letters, 8 (7), 2008, 2012.

A. Dato, M. Frenklach, Substrate-free microwave synthesis of graphene: experimental conditions and hydrocarbon precursors. New Journal of Physics, 2010, 12.12: 125013.

E. Tatarova et al. Microwave plasma based single step method for free standing graphene synthesis at atmospheric conditions. *Applied Physics Letters*, 2013, 103.13: 134101.

Graphene synthesis in volume at atmospheric pressure

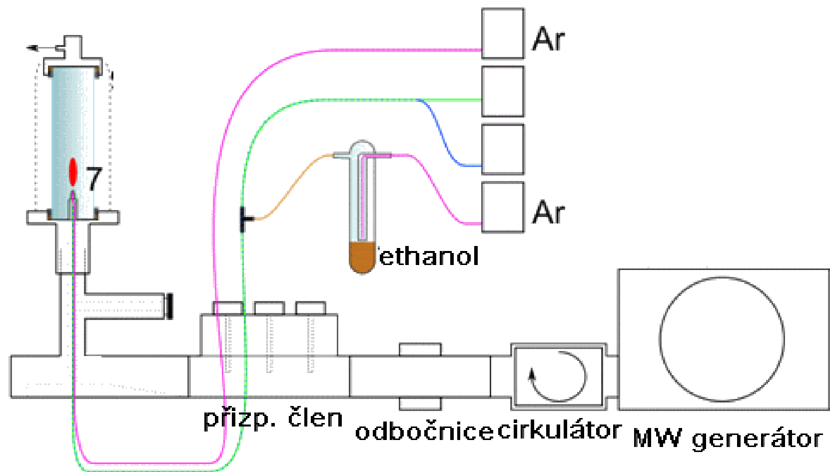

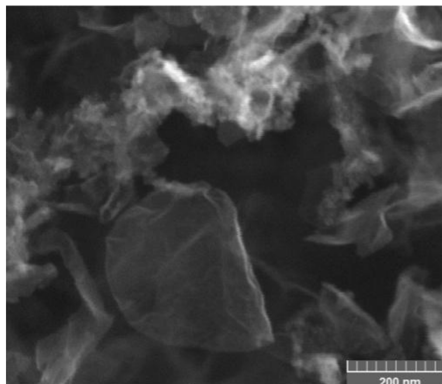

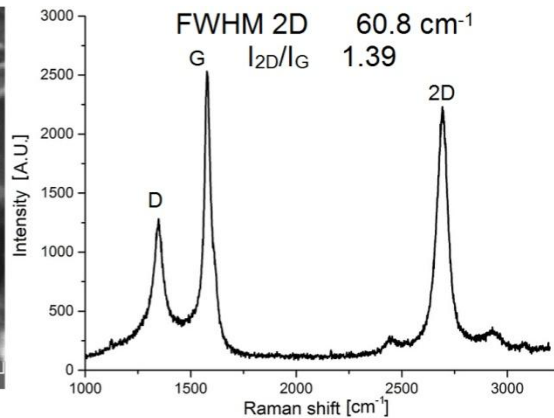

Graphene nanoribbons

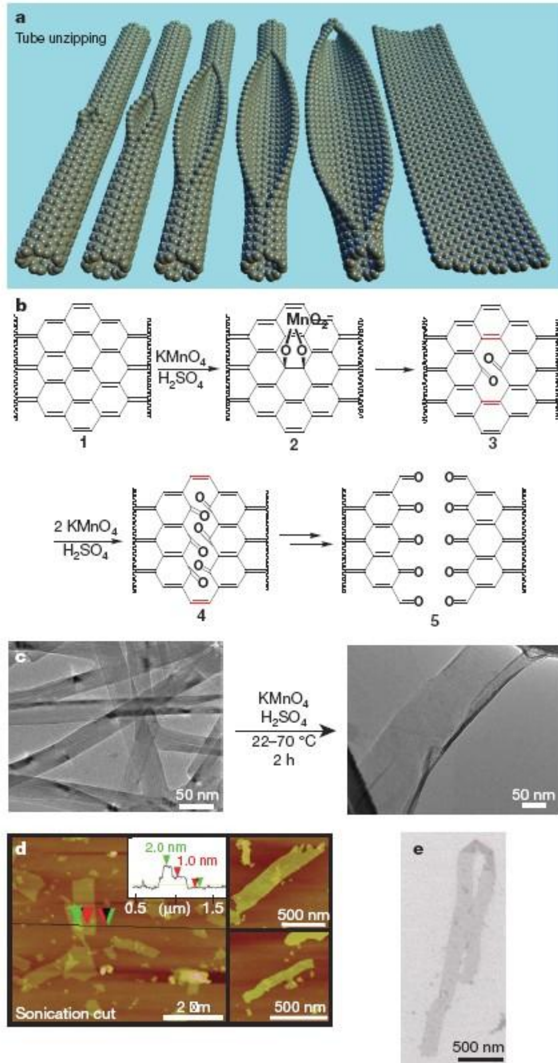

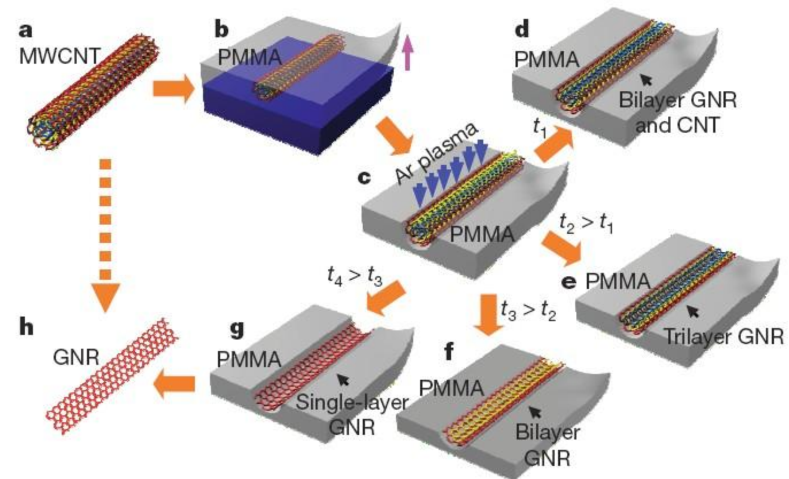

Figure 1 | Making GNRs from CNTs. a, A pristine MWCNT was used as the starting raw material. **b**, The MWCNT was deposited on a Si substrate and then coated with a PMMA film. **c**, The PMMA–MWCNT film was peeled from the Si substrate, turned over and then exposed to an Ar plasma. **d–g**, Several possible products were generated after etching for different times: GNRs with CNT cores were obtained after etching for a short time t_1 (**d**); tri-, bi- and single-layer GNRs were produced after etching for times t_2, t_3 and t_4, respectively ($t_4 > t_3 > t_2 > t_1$; **e–g**). **h**, The PMMA was removed to release the GNR.

Liying Jiao et al., Narrow graphene nanoribbons from carbon nanotubes, 458, Nature, 877.

Dmitry V. Kosynkin et al., Longitudinal unzipping of carbon nanotubes to form graphene nanoribbons, Nature, 458, 2009, 872.

P. Ruffieux et al., On-surface synthesis of graphene nanoribbons with zigzag edge topology, Nature, 531, 2016, 489.

GNR – zig-zag metallic, archmchair – metallic and semiconducting

Graphene transfer to dielectric substrate

- Graphene transfer scheme on Cu foil: a) PMMA mask b) etching of graphene on one side of the foil in O_2 plasma, c) chemical etching of Cu (for example in $FeCl_3$) d) transfer of PMMA+graphene to dielectric substrate e) chemical or plasma etching of PMMA.
- Gao, L. *et al. Nature* ***505, 190–194 (2014).***

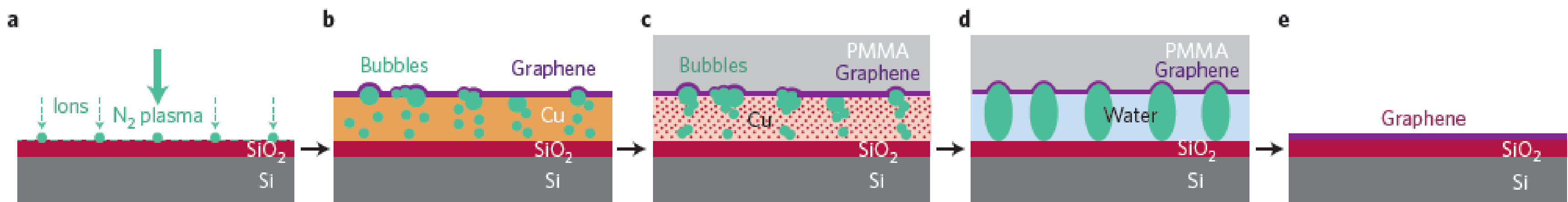

Literature

- M. Meyyappan, L. Delzeit, A. Cassell, D. Hash. *Plasma Sources Sci. Technol*. **12**, 205 (2003)
- M. Meyyappan, J. Phys. D: Appl. Phys. **42** (2009) 213001
- T. Nozaki, S. Yoshida, T. Karatsu and K. Okazaki, Atmospheric-pressure plasma synthesis of carbon nanotubes, J. Phys. D: Appl. Phys. 44 (2011) 174007 (9pp)
- Z. Bo et al., Plasma-enhanced chemical vapor deposition synthesis of vertically oriented graphene nanosheets, Nanoscale, 2013, 5, 5180.
- E. Tatarova et al. Microwave plasma based single step method for free standing graphene synthesis at atmospheric conditions. *Applied Physics Letters*, 2013, 103.13: 134101.
- X. Chen, B. Wu, Y. Liu, Direct preparation of high quality graphene on dielectric substrates, ***Chem. Soc. Rev., 2016,*** 45, 2057.
- Commercial presentations: AIXTRON Black Magic, Oxford Nanofab